Delayed recombination and cosmic parameters

Silvia Galli,[1] Rachel Bean,[2] Alessandro Melchiorri,[1] and Joseph Silk[3]

[1]*Universita' di Roma "La Sapienza", Ple Aldo Moro 2, 00185, Rome, Italy.*
[2]*Department of Astronomy, Space Sciences Building, Cornell University, Ithaca, New York 14853, USA.*
[3]*Astrophysics, Denys Wilkinson Building, University of Oxford, Keble Road, OX1 3RH, Oxford, UK.*

Current cosmological constraints from cosmic microwave background anisotropies are typically derived assuming a standard recombination scheme, however additional resonance and ionizing radiation sources can delay recombination, altering the cosmic ionization history and the cosmological inferences drawn from the cosmic microwave background data. We show that for recent observations of the cosmic microwave background anisotropy, from the Wilkinson microwave anisotropy probe satellite mission (WMAP) 5-year survey and from the arcminute cosmology bolometer array receiver experiment, additional resonance radiation is nearly degenerate with variations in the spectral index, n_s, and has a marked effect on uncertainties in constraints on the Hubble constant, age of the universe, curvature and the upper bound on the neutrino mass. When a modified recombination scheme is considered, the redshift of recombination is constrained to $z_* = 1078 \pm 11$, with uncertainties in the measurement weaker by 1 order of magnitude than those obtained under the assumption of standard recombination while constraints on the shift parameter are shifted by 1σ to $\mathcal{R} = 1.734 \pm 0.028$. From the WMAP5 data we obtain the following constraints on the resonance and ionization sources parameters: $\epsilon_\alpha < 0.39$ and $\epsilon_i < 0.058$ at 95% c.l.. Although delayed recombination limits the precision of parameter estimation from the WMAP satellite, we demonstrate that this should not be the case for future, smaller angular scales measurements, such as those by the Planck satellite mission.

I. INTRODUCTION

The recent measurements of the cosmic microwave background (CMB) flux provided by the 5 yr wilkinson microwave anisotropy probe (WMAP) mission [1,2] and the arcminute cosmology bolometer array receiver (ACBAR) collaboration [3] have confirmed several aspects of the cosmological standard model and improved the constraints on several key parameters. The constraints on the neutrino mass, for example, coming just from CMB data are drastically improved and are now competitive with current direct laboratory measurements (see e.g. [2,4]). Moreover, the presence of a neutrino background is now inferred at more than 95% c.l. by CMB data alone (see e.g., [2,5]). Finally, inflationary parameters, curvature, baryonic and dark matter densities are also now better determined due to improved treatment of systematics (see [2,6]).

These spectacular results, apart from the experimental improvements, have been possible due to the high precision of the CMB theoretical predictions that have now reached an accuracy close to 0.1% over a wide range of scales. A key ingredient in the CMB precision cosmology is the accurate computation of the recombination process. Since the seminal papers by Peebles and Zel'dovich (see [7,8]) detailing the recombination process, further refinements to the standard scheme were developed [9] allowing predictions at the accuracy level found in data from the WMAP satellite [10,11], even if uncertainties in the standard scenario may be large enough to pull parameters significantly for the Planck mission (see e.g. [12]).

While these crucial efforts towards the greatest accuracy on the recombination process are impressive, it should be noticed that these computations rely on the assumption of standard physics. nonstandard mechanisms such as (just to name a few) high redshift stars or active galactic nuclei, topological defects and dark matter decays could produce extra sources of radiation and modify the recombination process. With the WMAP results and the future Planck data, it therefore becomes conceivable that deviations from standard recombination may be detected.

Several papers in recent years have indeed investigated this possibility. For example, one could use a phenomenological approach such as in [13] or [14]. Other works have adopted a more physically motivated (but model-dependent) approach and considered modified recombination by allowing time variations in the fine-structure [15] or gravitational constants [16]. Here we instead focus on delayed recombination mechanisms based on the hypothesis of extra sources of ionizing and resonance radiation at recombination (see e.g. [17–19]).

Extra photon sources can be generated by a variety of mechanisms. A widely considered process is the decay or annihilation of massive particles [20–26]. The decay channel depends on the nature of the particles, and could, for example, include charged and neutral leptons, quarks or gauge bosons. These particles may then decay further, leading to a shower cascade that could, among other products, generate a bath of lower energy photons that would interact with the primordial gas and cosmic microwave

background. Interestingly these models, as well as injecting energy at recombination, boost the ionization fraction after recombination and can distort the ionization history of the universe at even later times, during galaxy formation and reionization [27–31]. Other mechanisms include evaporation of black holes [18,32] or inhomogenities in baryonic matter [18].

Several authors have already compared delayed recombination with cosmological data (see for example [33–37]). With respect to these previous analyses, we assess below the improvements given by more recent data from the WMAP 5 yr survey and from the ACBAR experiment. Moreover, we will study in detail the impact of delayed recombination on the current constraints on cosmic parameters. As showed in [17] delayed recombination has two main effects: damping of the CMB anisotropy and polarization at small angular scales and a shift of the acoustic peaks in their angular spectra. As we will see, these two effects change in a significant way the current constraints on such parameters as the spectral index n_S and the Hubble constant H_0. We then study the impact on the current determination of the redshift of recombination z_* and on the shift parameter $\mathcal{R}$. Both parameters are used to provide complementary geometric constraints on the background expansion history; $\mathcal{R}$ as a measure of the angular diameter distance to last scattering, and z_* in interpreting the scale of baryon acoustic oscillations [38,39], which in combination with supernova type Ia data, can impose constraints on the dark energy component (see e.g. [40–42]). Here we show that delayed recombination has decisive effects on the determination of these parameters. Finally, we discuss the implications of a modified recombination scheme for the Planck satellite.

The paper proceeds as follows: in section II we briefly describe the delayed recombination scheme. In III we analyze the latest CMB data and place new constraints on delayed recombination. Moreover, we forecast the constraints prospectively attainable by the Planck satellite mission, and study the impact that a modified recombination scheme can have on several key cosmological and astrophysical parameters. In IV we draw our conclusions and review their future implications.

II. A MODIFIED IONIZATION HISTORY

Following [7,8] we can model the evolution of the electron ionization fraction, x_e in a simplified manner for the recombination of hydrogen:

$$-\frac{dx_e}{dt}\bigg|_{std} = C\bigg[a_c n x_e^2 - b_c(1 - x_e)\exp\bigg(-\frac{\Delta B}{k_B T}\bigg)\bigg], \quad (1)$$

where x_e is the electron fraction per hydrogen nuclei, n is the number density of atoms, a_c and b_c are the effective recombination and photo-ionization rates for principle quantum numbers ≥ 2, ΔB is the difference in binding energy between the 1st and 2nd energy levels and

$$C = \frac{1 + K\Lambda_{1s2s}n_{1s}}{1 + K(\Lambda_{1s2s} + b_c)n_{1s}}, \qquad K = \frac{\lambda_\alpha^3}{8\pi H(z)}, \quad (2)$$

where λ_α is the wavelength of the single Ly-α transition from the $2p$ level, Λ_{1s2s} is the decay rate of the metastable $2s$ level, $n_{1s} = n(1 - x_e)$ is the number of neutral ground state H atoms, and $H(z)$ is the Hubble expansion factor at a redshift z.

As in [34], we include the possibility of extra photons at key wavelengths that could modify this recombination picture, namely, resonance (Ly-α) photons with number density, n_α, which promote electrons to the $2p$ level, and ionizing photons, n_i, [17–19,33]

$$\frac{dn_\alpha}{dt} = \varepsilon_\alpha H(z)n, \qquad \frac{dn_i}{dt} = \varepsilon_i H(z)n, \quad (3)$$

where ε_α and ε_i are assumed constant with redshift.

This leads to a modified evolution of the ionization fraction

$$-\frac{dx_e}{dt} = -\frac{dx_e}{dt}\bigg|_{std} - C\varepsilon_i H - (1 - C)\varepsilon_\alpha H. \quad (4)$$

These are additional production rates over and above those in the standard scenario.

We employ the widely used RECFAST code [9], in the cosmomc package [43] modifying the code as in (4) to include two extra constant parameters, ϵ_α and ϵ_i.

The effects of delayed recombination on the primordial power spectra have been thoroughly investigated by [17]. Namely, the main consequences are damping of CMB anisotropies and polarization on small angular scales and a shift of the acoustic peaks towards larger scales. This introduces a main degeneracy with two parameters: the scalar spectral index n_S and, in a flat universe, the Hubble constant H_0. In Fig. 1 we indeed plot anisotropy, polarization and cross temperature-anisotropy power spectra for two degenerate models. As we see, when delayed recombination is included, the degenerate spectra have a larger spectral index to compensate the damping and a smaller Hubble parameter to compensate the shift. This degeneracy will clearly appear as a correlation between the constraints on these parameters as we show in the next section.

We compare delayed recombination with current data by making use of the publicly available Markov Chain Monte Carlo (MCMC) package cosmomc [43]. Other than ε_α and ε_i, always taken as positive, we sample the following seven-dimensional set of cosmological parameters, adopting flat priors on them: the physical baryon and CDM densities, $\omega_b = \Omega_b h^2$ and $\omega_c = \Omega_c h^2$, the Hubble parameter H_0, the scalar spectral index, n_s, the normalization, $\ln 10^{10} A_s (k = 0.05/\text{Mpc})$, and the optical depth to reionization, τ. We also consider the possibility of having a curved universe with $\omega_k \neq 0$ [44] and three massive neutrinos each with same mass m_ν and overall energy density:
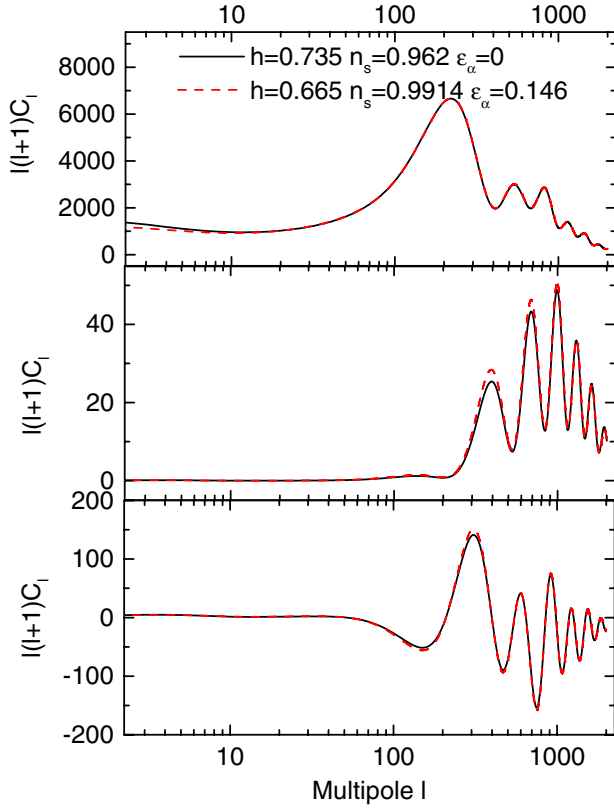
FIG. 1 (color online). Best fit WMAP5 Spectra and degenerate Anisotropy (Top), Polarization (Middle Panel) and cross Anisotropy-Polarization (Bottom Panel) angular power spectra in case of delayed recombination.

$$\omega_\nu = \frac{m_\nu}{30.8 \text{ eV}}. \tag{5}$$

We consider purely adiabatic initial conditions. In what follows we also consider bounds on two derived parameters: the recombination redshift z_* as defined in [17] and the "shift" parameter $\mathcal{R}$ defined as (see [40]):

$$\mathcal{R} = \frac{\omega_m^{1/2}}{\omega_k^{1/2}} \text{sinn}_k(\omega_k^{1/2} y), \tag{6}$$

where $\text{sinn}(x) = \{\sin(x), x, \sinh(x)\}$ for closed, flat and open geometries, respectively, with

$$y = \int_{a_*}^1 \frac{da}{\sqrt{\omega_m a + \omega_k a^2 + \omega_\Lambda a^4}}, \tag{7}$$

where $\omega_m = \omega_b + \omega_c$ and a is the scale factor with $a_* = (1 + z_*)^{-1}$. The MCMC convergence diagnostic tests are performed on 4 chains using the Gelman and Rubin "variance of chain mean"/"mean of chain variances" $R - 1$ statistic for each parameter. Our $1 - D$ and $2 - D$ constraints are obtained after marginalization over the remaining "nuisance" parameters, again using the programs included in the cosmomc package. We use a cosmic age top-hat prior as $10 \text{ Gyr} \leq t_0 \leq 20 \text{ Gyr}$. We include the

five-year WMAP data [2] (temperature and polarization) with the routine for computing the likelihood supplied by the WMAP team (we will refer to this analysis as WMAP5). Together with the WMAP data we also consider the small-scale CMB measurements of ACBAR [3] (we will refer to this analysis as WMAP5 + ACBAR).

III. LIKELIHOOD ANALYSIS AND RESULTS

A. Modified recombination with standard Λ-CDM

We first analyze the effects of modified recombination on the cosmological constraints obtained under the assumption of a flat, Λ-CDM model with massless neutrinos. After marginalization over the nuisance parameters described in the previous section, the WMAP5 data gives $\epsilon_\alpha < 0.39$ and $\epsilon_i < 0.058$ at 95% c.l. ($\epsilon_\alpha < 0.31$ and $\epsilon_i < 0.053$ when the ACBAR data is also included).

In Fig. 2 and 3 we plot the 68% and 95% c.l. likelihood contours on the $n_s - \epsilon_\alpha$, and $n_s - \epsilon_i$ planes for the WMAP5 and WMAP5 + ACBAR data sets, respectively. The figures highlight that even with the improved small scale CMB data, modified recombination's main effect is to drive n_s to higher values, reconciling the data with a $n_s = 1$, Harrison-Zel'dovich (HZ), spectrum, as was seen with the WMAP 3-year data [34]. Any conclusion on the compatibility of a particular inflationary model with the WMAP5 data, therefore, is highly dependent on the assumptions made on the recombination process and should be discussed with some caution in light of this.

Marginalizing over the recombination parameters we indeed get $n_s = 0.993^{+0.045}_{-0.040}$ (WMAP5 alone) and $n_s = 0.996^{+0.042}_{-0.038}$ (WMAP5 + ACBAR) at 95% c.l.., i.e. with $n_s = 1$ perfectly compatible with the data. Those results should be compared with the constraints $n_s = 0.959^{+0.026}_{-0.027}$ and $n_s = 0.965^{+0.027}_{-0.028}$ (95% c.l.) obtained using the same data sets and priors but with standard recombination.
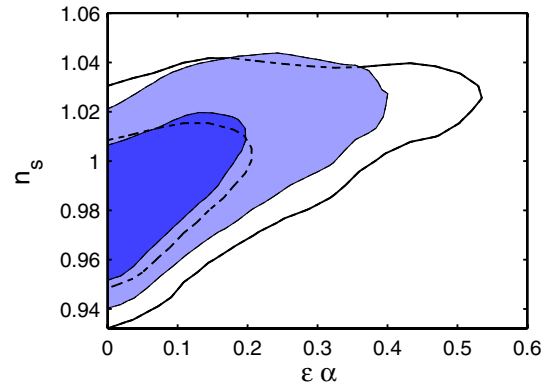

FIG. 2 (color online). Likelihood contours at 68% and 95% c.l. in the $n_s - \epsilon_\alpha$, plane for WMAP5 (empty contours) and WMAP5 + ACBAR (filled contours) experiments, respectively, allowing both ionizing and resonance radiation modifications to the recombination scheme.
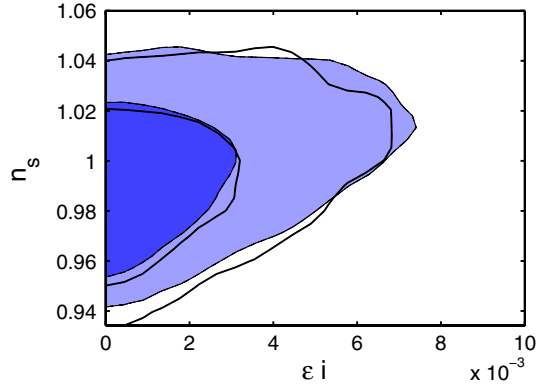
FIG. 3 (color online).   Likelihood contours at 68% and 95% c.l. in the $n_s - \epsilon_i$, plane for WMAP5 (empty contours) and WMAP5 + ACBAR (filled contours) experiments, respectively, allowing both ionizing and resonance radiation modifications to the recombination scheme.

As we can see from Fig. 2 it is possible to have $n_s = 1$ even if $\epsilon_\alpha = 0$. However this agreement, apparently in contrast with the standard WMAP5 result, is due to the marginalization over ϵ_i which is still present as a free parameter in the analysis. Since it may be possible to have only resonance radiation at recombination we analyze the effects of just varying ϵ_α while keeping $\epsilon_i = 0$. In Fig. 4 we plot the constraints on the n_s-ϵ_α plane with and without variation in ϵ_i. As we can see, when $\epsilon_i = 0$, the degeneracy between n_s and ϵ_α is more evident and HZ spectra are in well agreement at 1-σ level with WMAP5 only if additional ionizing radiation is present.

The degeneracy with the spectral index can be easily understood: delayed recombination suppresses the amplitude of the acoustic peaks in the CMB angular temperature anisotropy in a very similar way to an increase in the optical depth [17]. This effect can be compensated by an increase in n_s. Ionizing reionization also produces significant large angular scale polarization, and WMAP EE and TE constraints help to break the $n_s - \epsilon_i$ degeneracy.
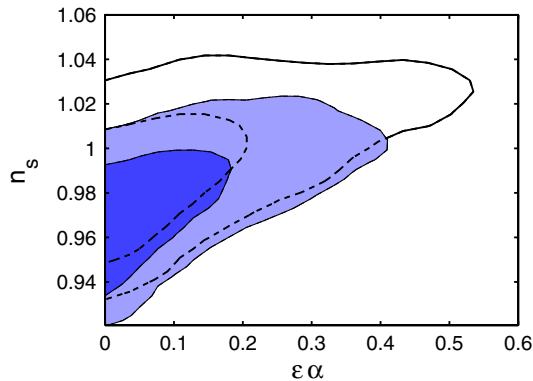

FIG. 4 (color online).   Likelihood contours at 68% and 95% c.l. on the $n_s - \epsilon_\alpha$, plane for WMAP5 assuming variations in ϵ_i (empty contours) and fixing $\epsilon_i = 0$ (filled contours).

However the same is not true for resonance recombination [34], and so the $n_s - \epsilon_\alpha$ degeneracy remains present despite improved polarization measurements.

Another effect of delayed recombination on the CMB spectrum, through the presence of resonance radiation, is a shift of the acoustic peak spectrum towards larger angular scales. An increase in ϵ_α shifts the epoch of recombination towards smaller z_*. This increases the size of the acoustic horizon at recombination and therefore shifts the peak towards smaller ℓ's (see [17,34],). In a flat universe, this effect can be counterbalanced by a decrease of the Hubble constant. In Fig. 5 (Top Panel) we plot the likelihood contours from WMAP5 on the $H_0 - \epsilon_\alpha$ plane. A degeneracy with the Hubble parameter is evident and the analysis yields $H_0 = 68.1^{+7.2}_{-8.6}$ at 95% c.l. that should compared with the value $H_0 = 71.9^{+5.2}_{-5.4}$ at 95% c.l. assuming standard recombination. Since smaller values of the Hubble constant are in agreement with larger ϵ_α it is easy to predict a correlation with the current age of the universe t_0.

In the bottom panel of Fig. 5 we plot the likelihood contours in the $t_0 - \epsilon_\alpha$ plane. As we see, larger values of ϵ_α are indeed in agreement with larger t_0. We find from WMAP5 that $t_0 = 14.0^{+0.6}_{-0.4}$ Gyrs to be compared with the constraint $t_0 = 13.7^{+0.3}_{-0.3}$ under standard recombination. Current CMB age constraints can, therefore, be underestimated if one assumes a standard recombination scheme.

The impact of delayed recombination on the remaining parameters is shown in Fig. 6 where we plot the 1-D likelihood functions for the optical depth τ and the baryon and cold dark matter densities ω_b and ω_c derived from the WMAP5 data with and without standard recombination. While the changes in the optical depth are minimal since this parameter is mainly fixed by large scale polarization data, delayed recombination may slightly bias the current constraints towards smaller ω_b and larger ω_c respect to the standard case.

Another parameter worthy of study, and on which the CMB usually provides clear and uncorrelated constraints, is the shift parameter, $\mathcal{R}$, (see eg. [41]) which defines the angular scale of the acoustic oscillations. The shift parameter is generally considered a simple, geometric way to implement information from CMB in determining constraints from independent data sets such type Ia supernovae or galaxy clustering. However this parameter is not directly measured by CMB observations but is essentially a by-product of the cosmological parameter inference based on CMB spectral data analysis, and most crucially the recombination history. Therefore, using the shift $\mathcal{R}$ to constrain cosmological parameters in combination with other data sets may suffer from model dependent assumptions. It is subsequently important to investigate the effects modified recombination can have on this key parameter. We find WMAP5 with delayed recombination constrains $\mathcal{R} = 1.737 \pm 0.028$ at 68% c.l., to be compared with $\mathcal{R} = 1.713 \pm 0.020$ at 68% c.l. for standard recombination.
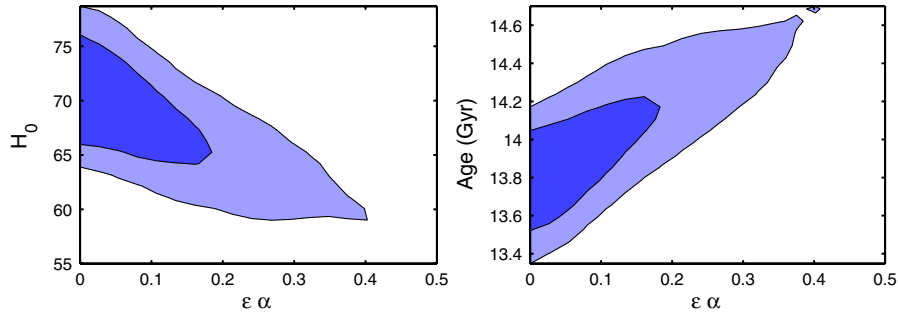
FIG. 5 (color online). Likelihood contours at 68% and 95% c.l. on the $H_0 - \epsilon_\alpha$, (top panel) and $t_0 - \epsilon_\alpha$ plane for WMAP5 fixing $\epsilon_i = 0$ (bottom panel). The Hubble constant is in units of km/s/Mpc.

Such a $1 - \sigma$ shift in $\mathcal{R}$ should not, however, alter in a significant way the current constraints on dark energy parameters derived from combined analyses assuming the standard recombination.

As expected, modified recombination strongly affects the constraints on the redshift of recombination, z_*. According to the latest WMAP5 results, the redshift of recombination z_* is $z_* = 1090.51 \pm 0.95$ with a better than 0.1% precision. However this impressive result is mainly driven by the assumption of standard recombination itself. With delayed recombination, we found $z_* = 1078.2 \pm 10.9$ at 68% c.l. from WMAP5 alone and $z_* = 1084.2 \pm 9.9$ with WMAP5 + ACBAR, so that the uncertainty in the measurement of z_* is increased by an order of magnitude.

In Fig. 7 we plot the 2-D likelihood contours for z_* and ϵ_α. A degeneracy following the relation $z_*(\epsilon_\alpha) \simeq z_*(0) \times (1 + 3\epsilon_\alpha)^{-0.042}$ (see [17]) is clearly evident and explains

why the constraints on z_* are much broader in the presence of delayed recombination.

B. Modified recombination with curvature

As mentioned in the previous section, delayed recombination decreases z_*, increasing the size of the sound horizon at recombination. This shifts the position of the acoustic peaks in the CMB spectrum as $\ell \sim (z_*/z_*^{standard})^{1/2}$. We therefore expect a degeneracy between ϵ_α and the curvature ω_k:, namely, a lower recombination redshift shifts the CMB peaks to larger angular scales (smaller ℓ's) yielding open models more consistent with the data (see [17]). However, as already pointed out in [17], measurements of the multiple peaks in the angular spectrum should break this degeneracy. In this section we perform an analysis of delayed recombination in curved
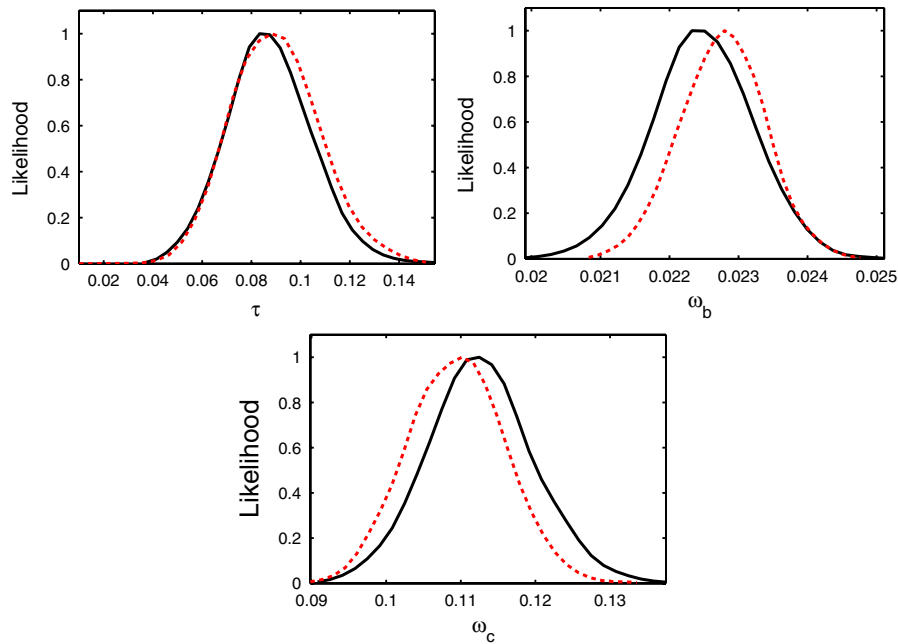

FIG. 6 (color online). Likelihood distribution function from WMAP5 on the optical depth (left top panel), the baryon density (right top panel) and the cold dark matter density (bottom panel). The red dashed line are the results assuming standard recombination, the solid black line are under the hypothesis of delayed recombination.
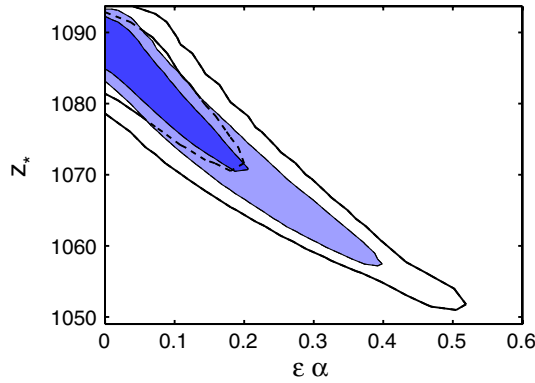
FIG. 7 (color online). Constraints on the z_*-ϵ_α plane from WMAP5 (empty contours) and WMAP5 + ACBAR (filled contours). A degeneracy along the relation $z_*(\epsilon_\alpha) = z_*(0) \times (1 + 3\epsilon_\alpha)^{-0.042}$ is evident.

models and check if a flat universe is still consistent with the data and test to what extent open models can be in agreement with observations. Including curvature, we found that the constraints on WMAP5 + ACBAR are slightly relaxed with $\epsilon_\alpha < 0.39$ and $\epsilon_i < 0.065$ at 95% c.l. However the effect on curvature from delayed recombination is small. Marginalizing over the recombination parameters we get $\omega_k = -0.033^{+0.058}_{-0.100}$ (WMAP5 + ACBAR) at 95% c.l.. to be compared with the constraint $\omega_k = -0.046^{+0.062}_{-0.094}$ obtained using the same data sets and priors but with standard recombination. The shifts towards open models due to delayed recombination is therefore at the level of few percent.

When external priors are added, we see little variation in the current constraints on Ω_Λ in a curved universe. We show this in Fig. 8 where we plot the usual constraints on the Ω_M-Ω_Λ but including delayed recombination. The changes are minimal respect to standard recombination. Adding a conservative prior on the matter parameter $\Omega_M =$
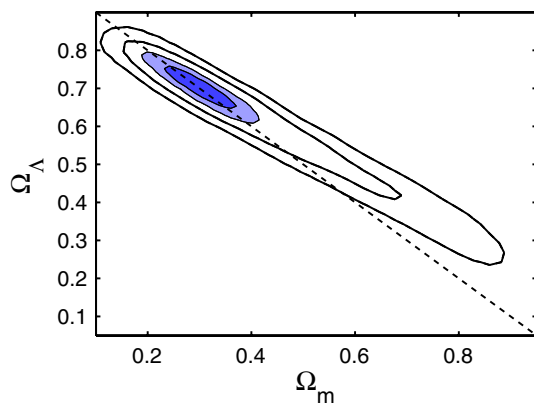

FIG. 8 (color online). Constraints on the Ω_M-Ω_Λ plane in the presence of delayed recombination from WMAP5 + ACBAR (empty contours) and after adding an external prior $\Omega_M = 0.30 \pm 0.05$ (filled contours). Dashed line is a flat Universe.

0.30 ± 0.05 motivated from galaxy clustering yields a constraint $\Omega_\Lambda = 0.70 \pm 0.04$ (to be compared with $\Omega_\Lambda = 0.712 \pm 0.037$ with standard recombination) still suggesting the presence of a cosmological constant at high significance.

C. Modified recombination and massive neutrinos

Cosmological neutrinos have a relevant impact on cosmology since they change the expansion history of the universe and affect the growth of perturbations. If neutrinos are nonrelativistic at recombination, CMB anisotropies can constrain neutrino masses indirectly since variations in the gravitational potential change the shape of the small scale CMB angular spectrum.

The recent WMAP5 data have provided an upper limit to the sum of neutrino masses of $\Sigma m_\nu < 1.3$ eV at 95% c.l. ([2]). Since this is the best upper limit current available on absolute neutrino masses from one single data set it is certainly timely to investigate how this bound could change when delayed recombination is included. We have found that from WMAP5 + ACBAR the bound on neutrino masses is $\Sigma m_\nu < 1.26$ eV at 95% c.l. under delayed recombination larger than $\Sigma m_\nu < 1.13$ eV obtained under standard recombination with the same data set and priors. We can therefore conclude that delayed recombination increases the current bound by $\sim 10\%$.

D. Forecasts for the Planck surveyor

In this section, we forecast the future constraints achievable on modified recombination from the Planck satellite experiment. We have constrained cosmic parameters assuming simulated Planck mock data with a fiducial model given by the best fit WMAP5 model (with standard recombination) and experimental noise described by

$$N_\ell = \left(\frac{w^{-1/2}}{\mu\text{K-arcmin}}\right)^2 \exp\left[\frac{\ell(\ell + 1)(\theta_{\text{FWHM}}/\text{arcmin})^2}{8\ln 2}\right],$$
(8)

with $w^{-1/2} = 63~\mu\text{K}'$ as the temperature noise level (we consider a factor $\sqrt{2}$ larger for polarization noise) and $\theta_{\text{FWHM}} = 7'$ for the beam size. We take $f_{\text{sky}} = 0.65$ as sky coverage.

With this configuration, we found the following constraints from Planck: $\epsilon_\alpha < 0.01$ and $\epsilon_i < 0.0005$ at 95% c.l., representing more than an order of magnitude in improvement in ϵ_α and 2 order of magnitude improvement in ϵ_i, respectively, in comparison to current WMAP5 + ACBAR constraints.

In Figs. 9 and 10 we show the effects of delayed recombination on constraining cosmological parameters from Planck. As we can see, the precision small scale temperature measurements of Planck markedly reduce the $n_s - \tau - \epsilon_i/\epsilon_\alpha$ degeneracies. ϵ_i is further constrained by small scale polarization measurements. Subsequently a modified
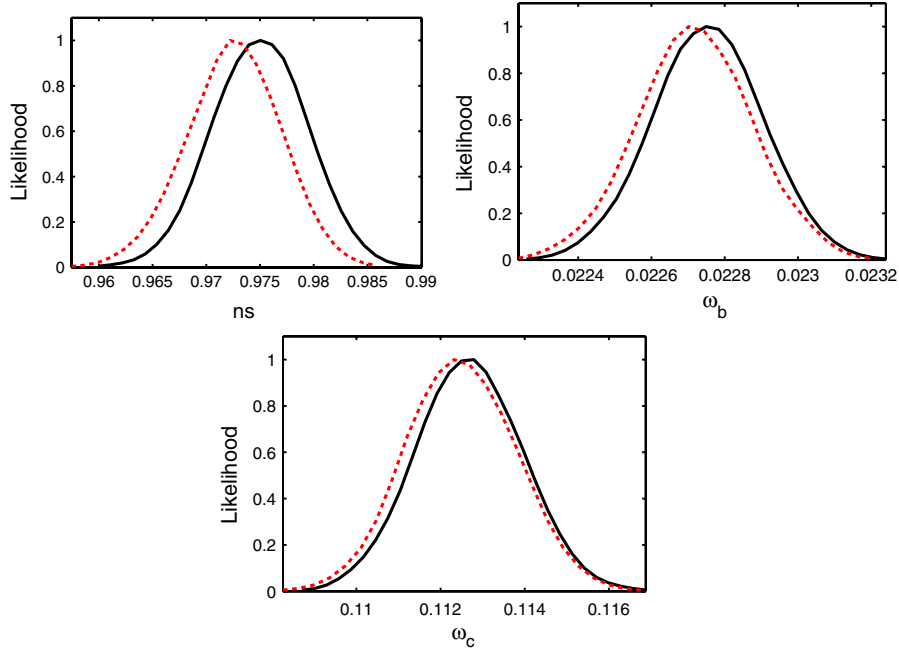
FIG. 9 (color online). Likelihood distribution function from a Planck-like satellite experiment (see text for the experimental configuration) on the scalar spectral index (top panel), the baryon density (center panel) and the cold dark matter density (bottom panel). The red dashed lines are the results assuming standard recombination, the solid black lines are under the hypothesis of delayed recombination.
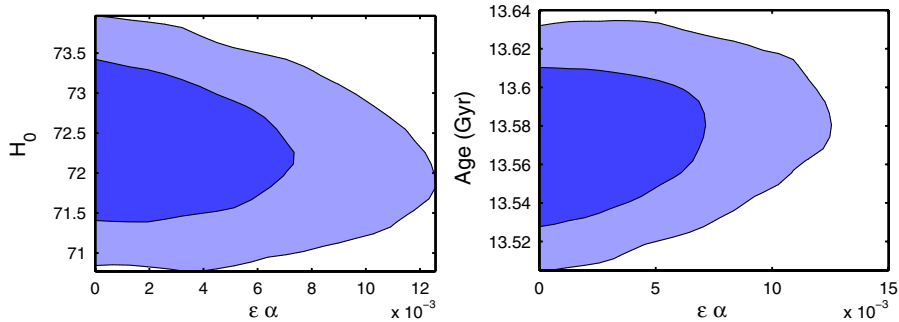

FIG. 10 (color online). 2D likelihood contour plots at 68% and 95% c.l. from a Planck-like satellite experiment (see text for the experimental configuration) for the Hubble parameter (top Panel) and age (Bottom Panel) versus the recombination parameter ϵ_α.

recombination scheme should result in values of the spectral index n_s being only slightly skewed towards more positive values in comparison to the standard scheme, and the Planck satellite will therefore be clearly able to discriminate n_s from a HZ spectrum with high significance even in the case of delayed recombination. The significantly larger uncertainties in t_0 and H_0 currently introduced if delayed, rather than standard, recombination is considered with the WMAP5 + ACBAR data would be significantly curtailed with Planck measurements.

IV. CONCLUSIONS

In this paper, we have updated the upper bounds that can be placed on the contribution of extra Ly-α and ionizing

photon-producing sources in light of the new WMAP and ACBAR data. We have found that, adopting a simple parametrization using constant, effective values for ϵ_α and ϵ_i, the WMAP5 data constraints $\epsilon_\alpha < 0.39$ and $\epsilon_i < 0.058$ at the 95% level (in a flat universe).

We have studied the implications of delayed recombination on several current cosmological constraints derived from CMB anisotropies. While we found no relevant changes on current CMB estimates of curvature, optical depth, baryon and cold dark matter densities, delayed recombination proves to have a significant impact on current constraints for inflationary parameters. Current conclusions for theoretical inflationary models, motivated by evidence for a deviation from scale invariance from recent

CMB data in the standard recombination scheme, would have to be relaxed when delayed recombination is considered, since the inflationary spectral index of scalar perturbations is in complete agreement with a scale invariant HZ spectrum.

The delayed recombination also has an impact on estimates of the shift factor, $\mathcal{R}$, and recombination redshift, z_*, currently used in estimating angular diameter distance and baryon acoustic oscillation measures of the cosmic expansion history. Moreover, constraints on particle physics parameters like the neutrino mass can also be relaxed when nonstandard recombination is considered.

Physically motivated models for nonstandard recombination, like those based on primordial black hole or super heavy dark matter decay, are possible and provide a good fit to the current data.

In particular, primordial black hole (PBH) decay [32] at the moment of recombination can be described by a model of the form

$$\varepsilon_j = c_j \zeta^{-(3/2)} \exp{-\zeta^{-(3/2)}}, \qquad \zeta = \frac{1+z}{1+z_{\mathrm{dec}}}, \qquad (9)$$

where j can be α or i and z_{dec} is the redshift of photon decoupling, where c_α and c_i are $\sim 10^{-1}$ but also depend on the inflationary spectrum of primordial perturbations [45] and on the possibility of accretion [46]. Note that in BH decay the models predict $\epsilon_i \sim \epsilon_\alpha$. The model presented in

[19] predicts $\epsilon_i \sim 10^{-5}$ in agreement with our current bounds.

The effect of a general particle decay can been described by the parameterization [19]:

$$\varepsilon_{\alpha,i} \sim \frac{10^{-8}}{\Omega_b^0 h^2} \Theta[z(t_x)](1+z)^r, \qquad (10)$$

with $r = 1/2$ for particle release from topological defects, $r = -1$ for decay of super heavy dark matter (SHDM), and where the normalization is the energetic gamma-ray experiment telescope (EGRET) energy density [47]. For short lived SHDM with $t_x < t_0$, $\Theta[z(t_x)] \sim \exp[(1 + z[t_x])^{3/2}]$ and equals 1 for all other cases. Our results on ϵ_i constraints $\Theta \leq 10^8$.

Future observations in both temperature and polarization, as those expected from the Planck satellite will be needed if we are to more stringently test and reduce the dependency of other cosmological parameters on delayed recombination models.

ACKNOWLEDGMENTS

---

[1] G. Hinshaw *et al.* (WMAP Collaboration), arXiv:0803.0732.
[2] E. Komatsu *et al.*, arXiv:0803.0547.
[3] C. L. Reichardt *et al.*, arXiv:0801.1491.
[4] G. L. Fogli *et al.*, Phys. Rev. D **78**, 033010 (2008).
[5] F. De Bernardis, L. Pagano, P. Serra, A. Melchiorri, and A. Cooray, J. Cosmol. Astropart. Phys. 06 (2008) 013.
[6] W. H. Kinney, E. W. Kolb, A. Melchiorri, and A. Riotto, arXiv:0805.2966.
[7] P. J. E. Peebles, Astrophys. J. **153**, 1 (1968).
[8] Ya. B. Zel'dovich, V. G. Kurt, and R. A. Sunyaev, Zh. Eksp. Teor. Fiz. **55**, 278 (1968); Sov. Phys. JETP **28**, 146 (1969).
[9] S. Seager, D. D. Sasselov, and D. Scott, Astrophys. J. **523**, L1 (1999).
[10] W. Hu, D. Scott, N. Sugiyama, and M. White, Phys. Rev. D **52**, 5498 (1995).
[11] U. Seljak, N. Sugiyama, M. White, and M. Zaldarriaga, Phys. Rev. D **68**, 083507 (2003)
[12] E. R. Switzer and C. M. Hirata, Phys. Rev. D **77**, 083006 (2008); C. M. Hirata and E. R. Switzer, Phys. Rev. D **77**, 083007 (2008).
[13] S. Hannestad and R. J. Scherrer, Phys. Rev. D **63**, 083001 (2001).

[14] A. Lewis, J. Weller, and R. Battye, Mon. Not. R. Astron. Soc. **373**, 561 (2006).
[15] S. Hannestad, Phys. Rev. D **60**, 023515 (1999); M. Kaplinghat, R. J. Scherrer, and M. S. Turner, Phys. Rev. D **60**, 023516 (1999); P. P. Avelino *et al.*, Phys. Rev. D **62**, 123508 (2000); R. Battye, R. Crittenden, and J. Weller, Phys. Rev. D **63**, 043505 (2001); P. P. Avelino *et al.*, Phys. Rev. D **64**, 103505 (2001); Landau, Harari, and Zaldarriaga, Phys. Rev. D **63**, 083505 (2001); C. J. A. Martins, A. Melchiorri, G. Rocha, R. Trotta, P. P. Avelino, and P. Viana, Phys. Lett. B **585**, 29 (2004); G. Rocha, R. Trotta, C. J. A. Martins, A. Melchiorri, P. P. Avelino, R. Bean, and P. T. P. Viana, Mon. Not. R. Astron. Soc. **352**, 20 (2004); C. J. A. Martins, A. Melchiorri, R. Trotta, R. Bean, G. Rocha, P. P. Avelino, and P. T. P. Viana, Phys. Rev. D **66**, 023505 (2002).
[16] O. Zahn and M. Zaldarriaga, Phys. Rev. D **67**, 063002 (2003).
[17] P. J. E. Peebles, S. Seager, and W. Hu, Astrophys. J. **539**, L1 (2000).
[18] P. D. Naselsky and I. D. Novikov, Mon. Not. R. Astron. Soc. **334**, 137 (2002).
[19] A. G. Doroshkevich, I. P. Naselsky, P. D. Naselsky, and I. D. Novikov, Astrophys. J. **586**, 709 (2003).

[20] S. Sarkar and A. Cooper, Phys. Lett. B **148**, 347 (1984).

[21] D. Scott, M. J. Rees, and D. W. Sciama, Astron. Astrophys. **250**, 295 (1991).

[22] J. Ellis, G. Gelmini, J. Lopez, D. Nanopoulos, and S. Sarkar, Nucl. Phys. **B373**, 399 (1992).

[23] A. J. Adams, S. Sarkar, and D. W. Sciama, Mon. Not. R. Astron. Soc. **301**, 210 (1998).

[24] A. G. Doroshkevich and P. D. Naselsky, Phys. Rev. D **65**, 123517 (2002).

[25] P. D. Naselsky and L. Y. Chiang, Phys. Rev. D **69**, 123518 (2004).

[26] L. Zhang, X. L. Chen, Y. A. Lei, and Z. G. Si, Phys. Rev. D **74**, 103519 (2006).

[27] E. Pierpaoli, Phys. Rev. Lett. **92**, 031301 (2004).

[28] X. L. Chen, and M. Kamionkowski, Phys. Rev. D **70**, 043502 (2004).

[29] N. Padmanabhan and D. P. Finkbeiner, Phys. Rev. D **72**, 023508 (2005).

[30] M. Mapelli, A. Ferrara, and E. Pierpaoli, Mon. Not. R. Astron. Soc. **369**, 1719 (2006).

[31] A. Lewis, arXiv:astro-ph/0603753.

[32] P. D. Naselsky and A. G. Polnarev, Sov. Astron. Lett. **13**, 67 (1987).

[33] R. Bean, A. Melchiorri, and J. Silk, Phys. Rev. D **68**, 083501 (2003).

[34] R. Bean, A. Melchiorri, and J. Silk, Phys. Rev. D **75**, 063505 (2007).

[35] J. Kim and P. Naselsky, arXiv:0802.4005.

[36] P. Stefanescu, New Astron. Rev. **12**, 635 (2007).

[37] L. Zhang, X. Chen, M. Kamionkowski, Z. g. Si, and Z. Zheng, Phys. Rev. D **76**, 061301 (2007).

[38] D. J. Eisenstein *et al.* (SDSS Collaboration), Astrophys. J. **633**, 560 (2005).

[39] W. J. Percival, S. Cole, D. J. Eisenstein, R. C. Nichol, J. A. Peacock, A. C. Pope, and A. S. Szalay, Mon. Not. R. Astron. Soc. **381**, 1053 (2007).

[40] G. Efstathiou and J. R. Bond, Mon. Not. R. Astron. Soc. **304**, 75 (1999).

[41] P. S. Corasaniti and A. Melchiorri, Phys. Rev. D **77**, 103507 (2008).

[42] O. Elgaroy and T. Multamaki, arXiv:astro-ph/0702343.

[43] A. Lewis and S. Bridle, Phys. Rev. D **66**, 103511 (2002) (Available from http://cosmologist.info.)

[44] In the case of curved models we consider the ratio of the sound horizon and angular distance at recombination parameter θ instead of H_0, modified accordingly to [17].

[45] A. R. Liddle and A. Green, Phys. Rep. **307** 125 (1998).

[46] R. Bean and J. Magueijo, Phys. Rev. D **66**, 063505 (2002).

[47] G. Bertone, G. Sigl, and J. Silk, Mon. Not. R. Astron. Soc. **326**, 799 (2001).